https://doi.org/10.15407/ufm.25.01.132

I.E. VOLOKITINA*, A.I. DENISSOVA,**
A.V. VOLOKITIN*, and E.A. PANIN******
Karaganda Industrial University,
Republic Ave. 30,
101400 Temirtau, Kazakhstan

* i.volokitina@alservice.kz, ** a.denisova@tttu.edu.kz,
*** a.volokitin@tttu.edu.kz, **** ye.panin@tttu.edu.kz

METHODS FOR OBTAINING A GRADIENT STRUCTURE

The methods for fabrication of the functionally-gradient materials, which have a high complex of unique mechanical, technological and special properties, when they working on impact, wear, fatigue, experiencing increased cyclic and alternating loads, are reviewed. Considered materials are used in aerospace engineering, energy, and other industries characterized by extremely unfavourable, extreme operating conditions of critical parts, structural elements, and assemblies. Different methods for fabrication of the gradient structures are considered, in particular, the method of severe plastic deformation of metals and the process of active bending of copper. The effect of grain size, texture, and grain-growth gradients on the deformation mechanisms and mechanical properties of gradient- nanostructured nickel, as well as functionally-gradient ceramic materials are studied. The review may be of interest to researchers and scientists in the field of materials science, metallurgy, and nanotechnology.

Keywords: gradient structures, functional-gradient materials, nanostructured materials, severe plastic deformation, mechanical properties of materials.

1. Introduction

Recently, metal scientists have been faced with the task of developing technological processes for obtaining materials with a high set of properties when working on impact, wear, fatigue, experiencing increased

Citation: I.E. Volokitina, A.I. Denissova, A.V. Volokitin, and E.A. Panin, Methods for Obtaining a Gradient Structure, *Progress in Physics of Metals*, **25**, No. 1: 132–160 (2024)

cyclic and alternating loads [1–10]. Graded materials have unique mechanical, technological and special properties. Functionally graded materials are a new class of materials that show a gradual change in mechanical properties or chemical composition with depth from the surface. Currently, for the manufacture of functionally graded materials, medium-carbon-alloyed high-strength steels are widely used, which have a high level of mechanical and technological properties. However, further increase in their properties and service life of parts based on them is hampered by several disadvantages of traditional heat treatment technologies [11–15]. Development of technical progress requires searching for new non-standard methods for obtaining materials with a gradient distribution of properties over the cross section, capable of operating under difficult operating conditions. Existing world experience has convincingly shown that the use of high-energy impact methods and their combination with traditional heat treatment technologies makes it possible to form a gradient structure of materials that provides an increased level of service properties of parts that best meet their operating conditions [16–18]. The analysis of literature showed that high-strength steels, aluminium and titanium alloys, and ceramics are currently widely used for the manufacture of functionally graded materials. Moreover, they are used both in the form of monolithic materials and multilayer composite materials with a gradient structure. Reports on the creation of layered materials with a gradient structure the front layer of which is made of solid materials and connected to a viscous back layer by rolling, welding, soldering, gluing, *etc.* are of great interest. At the same time, multilayer compositions have certain disadvantages, since they are prone to warping, delamination during thermal exposure and operation. There is information about the creation of a gradient structure on monolithic materials, in which the front surface of the product is strengthened to a certain depth, while the back part has high strength and toughness characteristics. This is achieved by using various processing methods: chemical-thermal treatment, surface hardening, surface alloying, application of various coatings and surfacing. At the same time, an obvious gap in previous studies is the poor development of materials science foundations for the influence of high-speed heat treatment modes on the structure, phase composition, and mechanical properties of medium-carbon high-strength steels used to create functionally graded materials. The features of high-strength alloy steels softening kinetics during tempering have not been sufficiently studied. Comprehensive studies are required to obtain functionally graded materials based on high-strength steels using high frequency, electric contact and laser heating or their combination with traditional technologies of thermal and chemical-thermal treatment.

2. Structural-Compositional Gradients: Basic Idea, Preparation, and Applications

The term 'gradient materials' refers to gradients of chemical composition and/or microstructural parameters that are deliberately introduced into components of any type of homogeneous or heterogeneous materials, including metal alloys, ceramics, glasses, polymers and composites.

Gradients in technical components have been well known since the beginning of material technology: we can mention carburized or nitride steels, composition distribution over welds, segregations and grain shape transitions in the alloy solidification, optical glass fibres with a radial refractive index gradient, ion exchange strengthened glass surfaces, metal surface layers modified by ion implantation, or p–n junctions in doped semiconductors. However, the concept of gradient materials as it is currently applied clearly refers to the introduction of engineering functions of the concentration profile and parameters based on desired profile and/or integral properties quantitative predictions. The second essential feature of modern gradient technology is the presence of reproducible manufacturing processes that accurately establish profile function resulting from analysis and calculation on the designer's desktop and at the same time viable on an industrial scale. These two factors: design of application-oriented profile and subsequent implementation of the desired graduated structure, can be considered like an introduction of gradients into the structural or functional component as an overall design tool, giving an additional degree of freedom for technical systems material optimization. Japanese scientists and engineers, who still play a leading role in this field, introduced the abbreviation FGM (functional gradient material), which is now commonly used [19].

The concept of gradient materials historically was first mentioned in international scientific journals in 1972, when the Massachusetts Institute of Technology named by metallurgist M.B. Bever published results of 'brainstorming' [20, 21]. Although Bever's work was funded by the US Advanced Research Projects Agency, there were no immediate actions and discovers. 10 years later, Gradient Metal Alloy Program at Michigan Tech. University at Houghton MI again led to a number of publications and conference presentations. At the same time, national commercial supersonic space shuttle develop program was launched in Japan; development of thermal barrier coating for this ambitious vehicle was the goal of a very large number of research program, that caused development of gradient materials. The first results were published only in Japanese, then from time to time in other international journals and conferences. The program quickly gained momentum and led to impressive results, which were presented in 50 out of 70 contributions to the 'First International Symposium on FGM' in Sendai

in 1990. At the same time, in Germany, Switzerland, France, Belgium, Finland, some laboratories began their independent activities, including study of gradient structures of materials [20–23].

Gradient structures can be formed both in the volume (bulk gradient states or gradient structural phase states) and on the surface (surface GSs or GSPSs). Volumetric ones include welds, diffusion and shock-explosive compounds, products of self-propagating high-temperature synthesis, deformation of localization zones. To surface gradient structures it is necessary to carry: arisen at friction or oxidation; formed as a result of saturation of the surface with various interstitial elements (carburizing, nitriding, boriding, *etc.*) or substitution elements (gold plating, silver plating, chromium plating, nickel plating, *etc.*); arising as a result of surface hardening or other methods of mechanical hardening of the surface; formed as a result of ultrasonic surface treatment; arising after exposure to shock waves, electron beams, powerful ion beams, intense plasma flows, due to laser exposure or exposure to powerful microwave radiation, as well as in gas discharge plasma; formed as a result of magnetron sputtering. Gradient structures arise not only as a result of various types of impact on the surface of material, but also with volumetric methods of material processing, for example, during forging, rolling, drawing, stamping, *etc.* Moreover, gradient structures distribution degree in this case can be even greater than with surface impact. Note that during rolling, gradient structures arise both in the rolled material and in the rolls of a rolling mill.

In gradient structures, as one moves away from the surface, such characteristics as the phase composition, the density of defects and their organization (substructure), sizes of cells, fragments, subgrains and grains change. At the same time, concentration of alloying elements and impurities changes in the same direction. Moving away from the surface effects on the temperature-velocity conditions of phase transformations change and, accordingly, the degree of completion of these transformations. At the same time, operational technological characteristics should change, such as hardness and strength, ductility and corrosion resistance, internal stresses and crack density, *etc.* Their change with distance from the surface can obey various laws, which are, as a rule, a consequence of the nonlinear behaviour of system. For nonlinear systems, gradient structures are typical, in which not only the magnitude of gradient, but also its sign can change with distance from the surface.

The ideal case of a compositional gradient material can be seen in the Cu–Ni binary alloy, because it has the property of unlimited solid-state solubility. This, of course, is a consequence of these two components similarity (atomic numbers 28 and 29, stable structure, small difference in the electronic structure, which explains ferromagnetism of nickel). Permissible concentration of any metal in the Cu–Ni system

is from 0 to 100%, which entails the absence of special thermodynamic effects. However, situation changes if solid solutions with limited solubility (such as Cu–Zn, Cu–Sn) are studied [24, 25].

Properties of gradient structures change dependently on the composition variation changes. The simplest case is a change in the lattice constants, which (under growth conditions close to equilibrium) induces a bending moment in the beam with a monotonic gradient, while this gives a central zone subject to tensile stress and two outer layers with a compressive stress state, or vice versa in the case of a symmetric gradient. This effect is enhanced if the gradient sample is subjected to temperature changes, since the coefficient of thermal expansion (CTE) usually depends on the local composition. This effect can find 'active' and 'passive' applications: for instance, in the blades of a thermal gas turbine. Fatigue damage occurs in a material of homogeneous composition due to the temperature gradient that occurs due to the exposure of blade surface to the flow of hot gas and inside of the blade with air-cooling. The use of a gradient composition that controls the CTE value within the blade cross section will help to avoid cracks. Another example leads to the consideration of the elastic modulus E as a function of the composition and resulting elastic stresses. Let us assume that Cu–Ni single crystal with an l-dimensional composition gradient is condensed or galvanically deposited on a Ni substrate. Ideally, subsequent layers will be formed under pressure, since their lateral interatomic distances should adjust to the layers of substrate, being in a stressed state with a corresponding excess of energy. As the voltage mismatch increases, system tends to assume a lower energy configuration by creating a specific dislocation pattern (of the same sign) that compensates for differences in lattice parameters. It should be noted that in the case of such a gradient, introduction of dislocations reduces the total strain energy, in contrast to the situation in homogeneous crystals, where each dislocation length unit increases the strain energy. Thus, neither annealing nor recrystallization can be expected if the temperature of such installations is increased. Of course, at a sufficiently high temperature, long-range diffusion processes will be activated [19].

The main reason for the introduction of gradients in materials science is the realization that, as a rule, a single material cannot be optimized with respect to combinations of mechanical, thermal and chemical stresses that given component may be subjected too. The complex task, as a rule, is even exacerbated by considerations of compatibility with the environment, availability and cost of raw materials, possibility of reuse, processing and biocompatibility. Typical case is represented by structural member exposed to very high heat flux, corrosive environments, erosive wear and particle irradiation. Technical answer to this situation is either surface modification or coating. The latter solution is

often more complex and costly, but on the other hand more efficient: both the core material and coating can be individually optimized without compromising their respective tasks. Problem area with this strategy is not two materials, which form component, but at the interface between them, more precisely: in strength and adhesion strength between substrate and coating. Adhesion at the substrate-coating interface, as well as at the bulk interface of two-component parts or in multilayer systems, suffers from two problems: poor bonding of two materials and residual stresses that develop during fabrication or heat treatment. It is true that some organic adhesives (for example, well-known epoxy resin) have an adhesive strength that is greater than the practical cohesive strength of any of adjacent materials; if they are applied and used at room temperature, there will be no serious internal stress problems. However, there are large and important applications where this type of adhesive joint is not practical due to temperature and other boundary conditions, so alternative solutions are required. The first response of materials engineers faced with the problems of mating two materials was to include an intermediate layer that helps create a specific transition. Often practical experience shows that this is not enough, so a second intermediate layer is applied. Following this design strategy logically leads to a multi-level concept with a step function of properties leading from material *A* to material *B*. Now, instead of trying to combine 2 or more individually different layers, we can also take it one step further and imagine a continuous function (with a gradient) leading from *A* to *B*. This can be achieved either by continuously changing the composition of solid solution or by continuously changing the volume fraction of two (or more) immiscible phases. Thermal barrier coatings are behind Japan's successful FGM program. Technical challenge was accommodating extreme transient heat flow during re-entry of the Space Shuttle. Temperature differences of the order of 1000°C must be maintained in 3 mm thick structural elements. Solution of this problem is based on the development of a sheet-like component gradually changing from 100% ceramic (PSZ) on the outside to 100% metal (austenitic steel) on the inside. These components were developed through a coordinated effort between research institutions and industry at the initiative of the National Aerospace Laboratory (NAL) [19].

It has been suggested that similar types of smooth ceramic-to-metal transitions may be useful in other areas of technology whenever high-energy beams collide with cold container walls: nuclear fusion, combustion, plasma, electron beating, and laser technology. Alternative two insoluble metal combinations, which are under investigation, include W–Cu as well as FGM TiB_2–Cu and have been proposed for N combustion nozzles. Bonding of metal with ceramics is of fundamental importance for many technologies, in particular, for electronic production.

This is a classic field of intermediate and 'activating' layers using graduated transitions. Connection technology in general, as well as on a macro scale (welding, soldering, and diffusion) is of paramount importance for the assembly of mechanical and electrical systems. Concentration profiles across welds appear as essential features of the process. 'Engineering', *i.e.*, systematic calculation and development of optimal concentration profiles contributes to improving the quality of welding. For example, production of equipment for power plants often involves welding of austenitic and ferritic steel components; industry is well aware of the role of transitions between these two types of steel. Metal-cutting and drilling tools are characterized by high localization and vibration, and mechanical stresses necessary for the formation of metal chips or separation of rock pieces should contribute to brittle fracture. High-speed work must be compromised with the need for heat dissipation and economic requirement for maximum tool life. WC–Co and Diamond-Co are respectively the base materials for these two operations. Careful design gradients in size, shape, and volume fraction of the abrasive component should increase the 'quality product' of cutting speed times tool life, as well as protect metal and non-metal components from corrosion, especially at high temperatures. Gas turbine blades, for example, are typically protected with multiphase intermetallic linings ('MeCrAIY'). Due to the large thermomechanical impact, wear problem is very serious. Obviously, this is a typical task for a gradient solution. As another example, amorphous carbon or C–C composites suffer at high temperatures due to a lack of oxidation resistance. While SiC is an effective protective layer, its lattice constant and expansion coefficient do not match well with those of carbon. However, graduated layers C–TiC–SiC can be successfully used as a contribution to solving the problem. High-quality gears and other functional components of mechanical engineering are important consumers of expensive alloy steels. It is possible to obtain better economy and quality of materials by introducing gradients, leaving alloy steel only in places where it is irreplaceable [19].

New concept of graded materials is finding acceptance among design engineers for structural or functional purposes, hence widespread industrial application is largely dependent on the availability of processes for the preparation of such components. Common feature of all processes is that they must have an element that somehow builds up: a concentration profile, either layer by layer in the case of '1-D-FGM' or dotted for a 3*D* graduated part. A continuously stepwise or at least staged process is the key to the production of FGM. Preparation of FGM is possible from the vapour phase: in principle, all CVD and PVD processes are applicable, although the number of materials that are suitable for this line is somewhat limited. Gradient is controlled by gas flow and/or temperature. Low speed is only applicable to thin layers. It is

possible to use segregation during the solidification of bulk melts or melt films: however, it is difficult to control melt concentration at the solidification boundary. Liquid dynamic solidification, *i.e.*, 'Osprey process' occurs when alloy melt is 'sprayed' by a jet of inert gas and directed to the target surface, where droplets are rapidly quenched and solidified. There are commercial pilot plants and production level plants with 2 gradient spray nozzles. However, this process is not easy to control. Typical product is a relatively large slab or ingot. If thin dimensions are required, it should be borne in mind that the formation of graduated materials is still an undeveloped technology. During thermal and plasma spraying, solid powder mixture can be converted into a liquid spray by heat transfer from a hot gas (flame) or from gas plasma. Solidification mechanism is similar to the Osprey process. The main advantage of spraying methods is the great know-how accumulated in the manufacturing industry and availability of high-performance equipment. Electrolytic deposition can be used for either surface coating or electroplating. Graduated sheets can be stacked and compacted, resulting in 'multigradient structures'. Powder metallurgy methods are very convenient for making gradients and can also be based on highly advanced technology. Problems essentially come down to two main points: how to get a gradient green body and how to sinter a gradient green body in one sinter. To solve the first problem, several solutions have been proposed and tested: the simplest of them is to replace gradient with a step function corresponding, for example, to 7 powder compositions, prepare these 7 mixtures and fill a vertical mould with them. Mixtures and subsequent filling of a vertical form these mixtures with given amounts. Another method uses the supply of powder through a capillary and x–y-table; in this way, even three-dimensional structures can be realized. In the centrifugal method, powder mixture is fed into the centre of centrifuge and directed towards the outer wall where the powder gradually forms a ring with the desired concentration profile. Powder sizing and activation have satisfactorily addressed the problem of sintering rate non-uniformity within the gradient. Binders are used to stabilize green bodies, allowing technologies similar to metal injection moulding to be applied. Self-heating synthesis (SHS) is an alternative to furnace sintering, using the enthalpy of formation of a number of intermetallic compounds, carbides, *etc.* from their elements. After ignition, the heat of reaction is sufficient to maintain sintering temperature of the sample. However, quality of the microstructure usually requires the application of pressure during or after sintering. Infiltration of liquid metal into a pre-sintered skeleton of a higher melting component is also a method for gradient materials obtaining. Powder mixture can be projected as a thin jet onto the target surface, where it collides with a precisely focused laser beam, sintered with the surface to form a solid body.

To become a reliable and widespread technology, gradient materials still need to be improved in several ways, such as:

• theoretical substantiation of structure-forming, mechanical and electromagnetic properties;

• development of several model applications with an experimental function, for example, ceramic–metal thermal barrier coatings;

• rationalization of many existing manufacturing methods in order to create fast, cost-effective and reliable production lines that can make FGM competitive in a market with low profit margins;

• creation of standardized methods for testing and monitoring of gradient materials [19, 22].

3. Formation of a Gradient Structure under the Severe Plastic Deformation

According to the data of Ukrainian and Japanese scientists' [23] joint studies, severe plastic deformation (SPD) methods are best suited for massive parts of nanostructured materials manufacturing. Equal-channel angular pressure (ECAP) methods [24–28] and high-pressure torsion (HPT) methods [29–31] are implemented by simple shear under uniform deformation without changing the cross-sectional dimensions of the sample. In the case of rolling (CE), shear deformations are localized in the near-surface layer of metal. Intensity of shear deformation in the near-surface layer depends on change in deformation parameters and friction conditions in the contact. Steel 65Г (0.65C, 0.3Si, 0.6Mn, 0.3Cr, 0.3Ni) was deformed by rolling. Transmission electron microscopy (TEM) was used to study "cross section" samples of deformed material gradient structure. The TEM study showed that a cellular substructure was formed in the near-surface layer. The depth of deformed layer is about 40 μm. Average cell size in the direction of cross section is about 100–200 nm. It was found thin layer of nanostructure with a cell size of about 20–30 nm. According to scientists' opinion, such a substructure is formed due to the action of 'good' impurities.

Severe plastic deformation is the most preferred method for creating a nanocrystalline structure in a macroscopic volume. Traditional methods of deformation (elongation, compression, rolling, stretching, *etc.*) provide such an opportunity on a very thin samples (thin foil or wire). Comparison of the mechanical properties of materials with different degrees of deformation is difficult due to the scale effect. The most thorough study of the strain hardening of Fe-Armco at a high degree of deformation was carried out according to Ref. [32] on wire samples.

The creation of new high-strain methods is promising both for the development of the theory of strain hardening and for the design of structures of deformable materials. The Equal Channel Pressure Angle

(ECAP) method was developed by in Ref. [33]. Simple shear uniform deformation of high intensity can be achieved in a $15\times15\times150$ mm macro sample without changing its dimensions. Deformation without resizing makes it possible to carry out repeated operations in different directions of deformation and, as a result, control the process of structure formation at high temperatures.

Another method based on deformation according to the spiral extrusion (SE) scheme was proposed in Ref. [34]. In this case, the regime of simple shear deformation was also implemented. According to the model of structural evolution reported in Ref. [35], the static and dynamic recovery are the main reasons limiting the minimum dimensions of structural elements in a material at large deformations. On the one hand, many cells are lost from the structure during this process; on the other hand, recovery process contributes to the improvement of boundaries and increases disorientation of cells. However, this model cannot explain existence of deformation critical degree, which characterizes beginning of this process significant activation.

The disclination model of severe plastic deformation proposed in Ref. [36] is based on the analysis of micromechanical stress arising around a dislocation during plastic deformation. According to this, model plastic deformation in crystals is developed during the motion of dislocation at low and medium strains. However, after the transformation of substructure from the dislocation forest into the cells at $e_i \approx 0.2$, deformation mechanism is changed, and strong deformation is caused by the formation of disclination regime without decrease in the subgrain size. Theoretical calculation within the disclination model yields a critical cell size of ≈0.2 μm for b.c.c. metals. Since critical cell size depends on some physical constants (Burgers vector, elastic modulus, stacking fault energy), for some f.c.c. metals, its value is much lower. This agrees well with the latest experimental data [37, 38] obtained on Ni and Al deformed by ECAP, from which it can be seen that average size of structural element is 30–50 nm. Both the recovery model and disclination theory give very pessimistic predictions of the usefulness of severe plastic deformation methods for further reducing of subgrain size to a few nanometers. However, many experimental works [39–44] demonstrate nanostructure in deformed state, and in particular, near-surface layers obtained by mechanical milling or high-speed friction processing with a grain size of 1–10 nm. Dispersion of substructure and hardening of near-surface layers occur after dynamic sonication or the multiple damping methods [42]. Such layers have a very high level of microhardness.

It was shown in Ref. [39] that high-speed friction of Armco-Fe, which occurs simultaneously with blasting of surface with gaseous ammonia, promotes the formation of nanostructured layers (subgrain size

3–5 nm) with a depth of 200 μm and H_μ = 13000 MPa (yield strength of about 4000 MPa). The x-ray diffraction analysis shows high nitrogen content in the surface layer. The same strong dispersion of the structure (d = 5 nm) was observed in Ref. [40] after milling a powder of pure fine-grained iron (0.2 wt.% oxygen) for 60 h in a vacuum. In this experiment, nanostructural state was preserved after cold-pressing consolidated powder, but sintering at 1100 °C promotes recrystallization of nanostructure. After processing, this material had a grain size of 30 μm and 10% Fe_2O_3 particles. Probably, added oxygen penetrates into Fe powder through free surface of fine powder, despite the vacuum protection. As showed in Ref. [41], the mechanical milling (MM) is a more preferable hardening process than ECAP or cold rolling. It should be noted that iron powder can be significantly strengthened by MM treatment, and hardness of MM iron powder easily exceeds HV = 3.6 GPa (maximum for ESAP deformation) and, after 360 ks, MM treatment hardness of iron powder reaches about HV = 10 GPa and is almost equal to the hardness of cementite (Fe_3C). This hardness value translates into yield strength of approximately 3500 MPa. Inside the iron powder, new fine crystal grains are formed when processed by the MM method of the dynamic continuous recrystallization mechanism. Grains 10–30 nm in size are clearly observed in the dark-field image. X-ray diffraction analysis gave an average grain size of 25 nm. Although the existence of a disclination structure has been confirmed in some grains, it is certain that ultra-finishing a grain to such a nanoscale level results in noticeable hardening down to about HV = 10 GPa. Despite the increase in the number of structural studies, the nature and operation of deformation mechanisms in these structures remain open. Authors of Refs. [42, 43] proposed a new surface mechanical abrasion (SMA) method, where repetitive multidirectional plastic deformation in the surface layer of the sample was caused by the impact of flying balls. Directions of balls impact on the surface of sample are rather random due to the random directions of balls flight inside the vibration chamber. As a result of this treatment, grain refinement is observed in the surface layers, and the upper layer consists of ultrafine crystallites. Experiments have shown that nanocrystals with a grain size of circa 10 nm can be obtained in a ball mill and in SMA processing of metals, in which significantly higher strain rates (at comparable strains) are used compared to ECAP and rolling processes. New alternative approaches to functional surface structures using nanostructure-selective reactions due to a significant increase in atomic diffusion and chemical activity of the nanostructured surface layer are presented in Ref. [45].

An ultrafine gradient structure in near-surface layers can be obtained by axisymmetric drawing and with a help of twisting method. Optimal lubricant additives are used to optimize grain boundary struc-

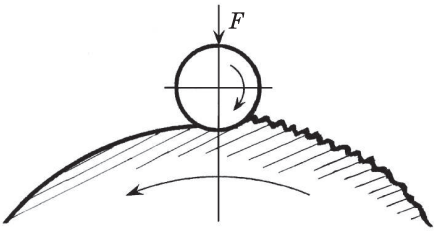

Fig. 1. Rolling technology sketch with a ball [23]

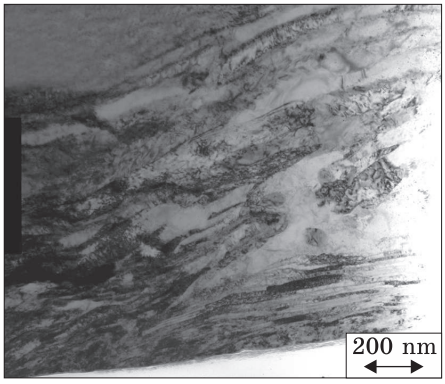

Fig. 2. Gradient structure of the bent steel sample after rolling [23] ▶

ture. Two main reasons explain such a high dispersion of the substructure: firstly, metal surface layers undergo much greater deformation under repeated intense dynamic impacts than after any static deformation method; secondly, near-surface deformation occurs in the presence of a special gas or optimal lubricant that penetrates material. Interaction between dislocation and added atoms suppresses reduction process and, consequently, reduces subgrains size. This mechanism is autocatalytic in the nature: structural dispersion accelerates diffusion of additive element into the depths of metal and increases its density, promoting structural dispersion. The important role of deformation temperature in the evolution of structure formation should be emphasized. Since dynamic deformation is accompanied by heating of the sample, there is an optimal temperature regime when the maximum structural dispersion is appeared. From [42] it follows that with deformed friction Armco-Fe, dispersion effect increases sharply at a test temperature of more than 300 °C. This is temperature of dynamic strain aging, when dislocation speed and diffusion speed of additional elements are approximately equal.

For the purpose of carrying out the experiment, authors of [23] used a cylindrical sample with a diameter of 50 mm made of steel 65Г (0.65C, 0.3Si, 0.6Mn, 0.3Cr, 0.3Ni) for deformation profiling. Rolling technology scheme is shown in Fig. 1 [23]. The hard alloy ball was placed on a special holder. This tool was pressed against the specimen with a fixed load of 100 N. The cylinder and the ball rolled at the same linear speed. Surface shear deformation is localized in the surface layer of the sample. The size of deformed zone depends on the load F, size of sphere, hardness of tool, workpiece material, rotation speed, etc. As a result of this treatment, there is a significant increase in hardness and decrease in surface roughness. Profiling allows reducing wear resistance of the developed parts by 5–6 times. Apparently, the main reason for such effects is related to the evolution of structure in the near-

surface zone. 'Cross-section' method was used to study gradient structure of deformable material. Two pieces of processed samples (3 mm long and ≈2.6 mm wide) were fastened together face to face, and then this block was built into a 3 mm diameter tube. For better fixation of tube and block, samples were glued together. This cylinder has been mechanically ground and polished. The other side was then sanded, leaving a final thickness of 120 μm. The disc was then indented on one side using 3 μm and 1 μm diamond paste. When central region of the sample reached thickness of 20 μm, dimple formation was stopped. Electronic transparency was achieved by ion milling on both sides using a state-of-the-art machine ion polishing system. Microstructure of cross-sectional samples was examined using a Philips C200 microscope operating at 200 kV. Gradient structure after rolling is shown in Fig. 2. Two zones of deformed structure are distinguished: a near-surface zone with a cellular structure of 20–30 nm and an internal zone with a coarse-cell structure (100–200 nm). According to Ref. [23], the ultrafine structure in the near-surface region is associated with the influence of interstitial impurities on the mechanism of structure formation. Near-surface deformation occurs when air or lubricant penetrates the material. Dislocation interactions and added atoms slow down reduction process and, as a result, reduce subgrain size. In this case, gas atoms suppress dynamic reduction process. Positive effect of interstitial impurities on the formation of nanostructure and mechanical properties was presented in [37, 38].

Changes in the temperature-speed regimes of deformation and chemical composition of elements that take part in the process of structure formation determine the dimensions of structural elements and layer thickness.

Thus, rolling makes it possible to obtain a gradient structure. The thickness of deformed layer reaches up to 40 μm. The cell size in this layer is 100–200 nm. In a heavily deformed near-surface layer (thickness ≈1 μm), where the effect of impurities is higher, cell size is 20–30 nm. Positive role of impurities in the formation of fine structure can manifest itself in strengthening the cell boundaries and improve performance of deformable materials.

4. Gradient Structural States in Copper after Active Bending

In the modern world, there is an increasing need to create promising industrial methods that allow achieving improved material properties. The most effective methods are IPD [46–50]. However, their development is hampered by the low technology of the proposed technical solutions, especially for the production of mass products. In this regard, the

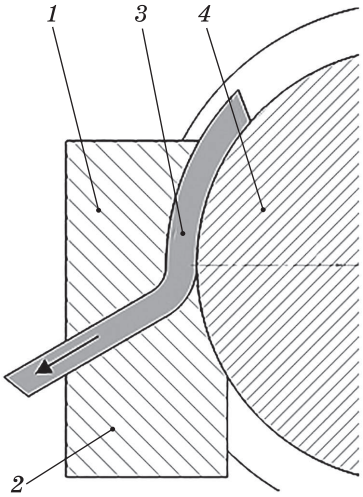

Fig. 3. Schematic diagram of the sample bending due to active friction force according to the 'Conform' sketch in a stationary bending matrix. Here, *1* and *2* denote two elements of the bending matrix, *3* is a sample, and *4* is a drive roller with engraving [51]

article considers the active bending method based on the use and advantages of 'Conform' scheme [51]. Its main advantage is the improvement of tribological situation in the process, which ensures the formation of ultrafine-grained (UFG) gradient structures of the product with increased wear resistance and plasticity at high strength values. The object of study was a long rod of commercially pure copper. The schematic diagram of active bending used in the research is shown in Fig. 3 [52]. The proposed development is based on the well-known ECAP 'Conform' scheme, and in the deformation process, the workpiece 3 is pushed into a stationary bending matrix, consisting of two elements of the matrix 1, 2 due to active forces friction drive roll with engraving 4. The technique can combine the high-performance 'Conform' process with bending deformation, which leads to a significant intensification of the hardening process, especially near-surface layers of the deformable material due to the formed composition. Active friction forces ensure process continuity. For modelling, 3D Deform program was used, designed to analyse the three-dimensional (3D) behaviour of the metal in the processes of forming. This made it possible to obtain important information about the nature of the material flow in the forming tool, stress–strain state and temperature distribution during the deformation process. When modelling bending according to 'Conform', a scheme at an angle of 90°, a square section blank 10×10 mm and more than 150 mm in length was used for the first cycle of deformation, bending radius 10 mm. For subsequent cycles, the sample obtained from the simulation of the previous cycle was used to obtain aggregated data after going through four cycles of sample processing.

The virtual experiment and its analysis showed that during processing, maximum strain intensity values are observed on the surface of the workpiece when bending at an angle of 90°. So, after one cycle in the upper part of the workpiece, the intensity of accumulated deformation reached $e = 1.04$ and in the lower part $e = 0.88$ and increased in proportion to the number of passes of the sample through the deforming channel (Fig. 4, *a*, *b*) [53].

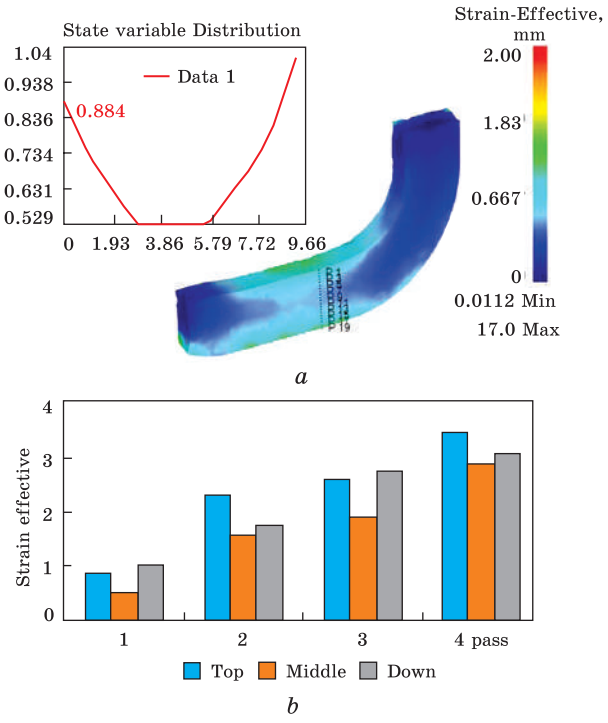

Fig. 4. Sample deformed state after the first cycle of bending at 90° (*a*) and the diagram of the intensity of deformation accumulated over the workpiece section after four passes (*b*) [52]

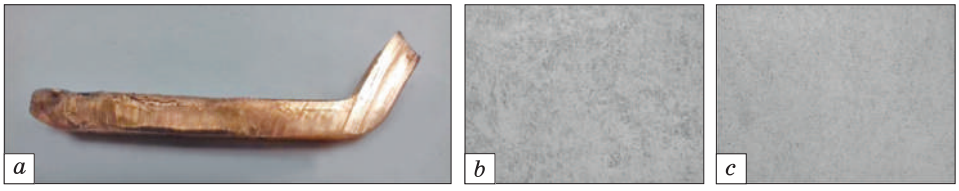

Fig. 5. General view of the sample subjected to the active bending (*a*), structure of the middle cross-sectional zone of the sample (OM) (*b*), and structure of the cross-sectional area of the workpiece (OM) (*c*) [52]

Plastic deformation makes it possible to obtain gradient compositions and deformable materials. Thus, in the subsequent analysis of the accumulated strain in the process of bending at an angle of 90°, it can be seen that with the increase in the number of bends, accumulated strain also increases. So, after four cycles of deformation treatment, the accumulated strain $e = 2.8–3.5$ for an angle of 90°, with the maximum value of the accumulated strain observed in the near-surface region of the deformed sample, and lower values in the middle region. The results of laboratory studies to obtain experimental samples and structural studies are presented in Fig. 5 [53]. It has been established that a finer-grained subgrain structure is formed in the surface layers.

It has been established that when using the active bending method, a gradient of grain–subgrain structure in the UFG range is formed in a deformed copper sample. The use of virtual modelling has shown that the bending method according to the 'Conform' scheme provides, after 4 processing cycles, a level of accumulated strain $e = 2.8$ in the middle region and $e = 3.5$ in the near-surface region of the cross-section of the sample [52].

5. Influence of Gradients of Grain Size, Texture, and Ability to Grow Grains on the Mechanisms of Deformation and Mechanical Properties of Graded Nanostructured Nickel

Complete understanding of the structure-property relationship of graded nanostructured metals is critical to the technological progress that will overcome barriers to engineering applications of this new class of materials with superior mechanical properties. Individual influence of three unique structural features, namely grain size gradient, texture gradient and grain-growth ability gradient, on the deformation mechanisms and mechanical properties of graded nanostructured nickel is investigated using the ultimate crystal plasticity based on dislocation density [53].

As found in Ref. [53], the growth of gradient grain size, which increases the relative proportion of large grains, leads to limited variations in the density of statistically stored dislocations (SSD), but a significant decrease in the density of geometrically necessary dislocations (GND) due to the different origin of these dislocations of the two grains, which leads to a significant weakening of traverse hardening, in contrast to moderate changes in the forest hardening of dislocations. Increasing texture gradient, which multiplies the sample's average Schmid's factor, results in successive decreases in SSD density, GND density, reverse stress and yield stress. The decrease in SSD density is associated with a decrease in the average shear-strain rate due to the Schmid's effect, while this effect and decrease in intergranular misorientation contribute to a decrease in GND density and reverse stress. In addition, an increase in the grain-growth ability gradient leads to an increase in SSD density due to a decrease in dislocation recovery, as well as a decrease in GND density and reverse stress due to a decrease in the strain gradient intensity. Strain localization decreases with increasing grain size gradient and texture gradient. These findings play an important role in optimizing of metals mechanical properties with a gradient nanostructure, as well as in the development of new heterostructured materials with exceptional properties and characteristics.

Traditionally, most metals and alloys for structural purposes are characterized by a homogeneous ((dis)ordered bulk [54–56] or nanosize

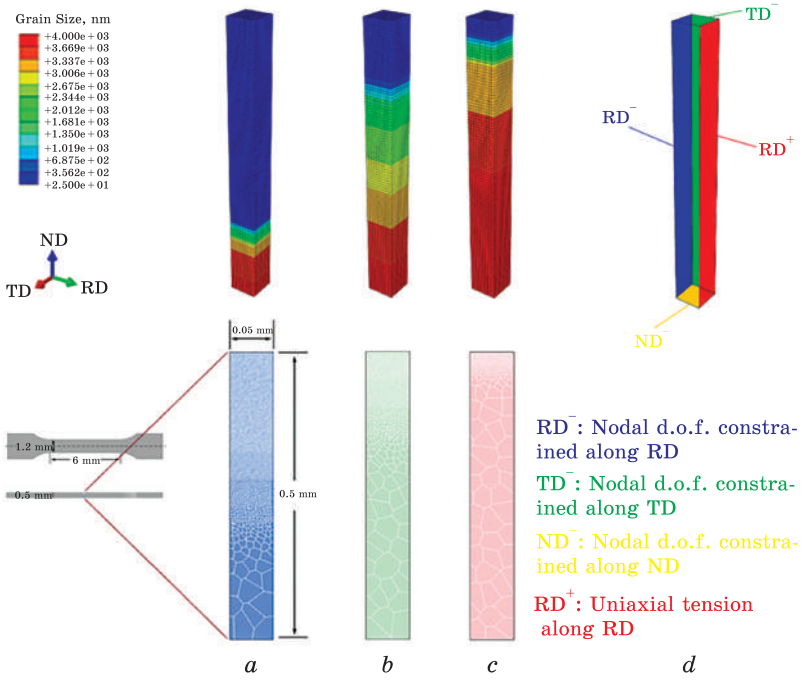

Fig. 6. The finite element models of 3 studied graded nanostructured Ni samples (*a*–*c*) and boundary conditions applied to the models (*d*). Schematic illustrations of the respective microstructures of the samples I (*a*), II (*b*), and III (*c*) are depicted below (*a*–*c*) [53]

[57–61]) microstructure with uniform average grain sizes in different parts. According to the classical Hall–Petch relation [53], a homogeneous polycrystalline metal can be strengthened by reducing average grain size, since an increase in the volume fraction of grain boundaries will further impede the movement of dislocations. However, decrease in grain size will inevitably lead to a decrease in the ductility and deformability of the material due to the limited mobility of dislocations, thus creating a dilemma known as the 'strength–ductility trade-off', which limits application of many metallic materials. However, in recent years, graded nanostructured metals (GNMs) have emerged as a new class of structural materials with promising potential to overcome the compromise between strength and ductility.

Finite element models of three studied samples (Figs. 6 and 7) with a gradient nickel nanostructure: *a* — sample I, *b* — sample II, and *c* — sample III with different grain size gradients, as well as schematic illustrations of their microstructures [53]. Each model consists of 10 000 C_3D_8 elements. Sample I has the mildest grain size gradient, while sample III has the steepest. The three illustrations of GNM nickel samples below the three finite element models are only schematic and symbolic. They

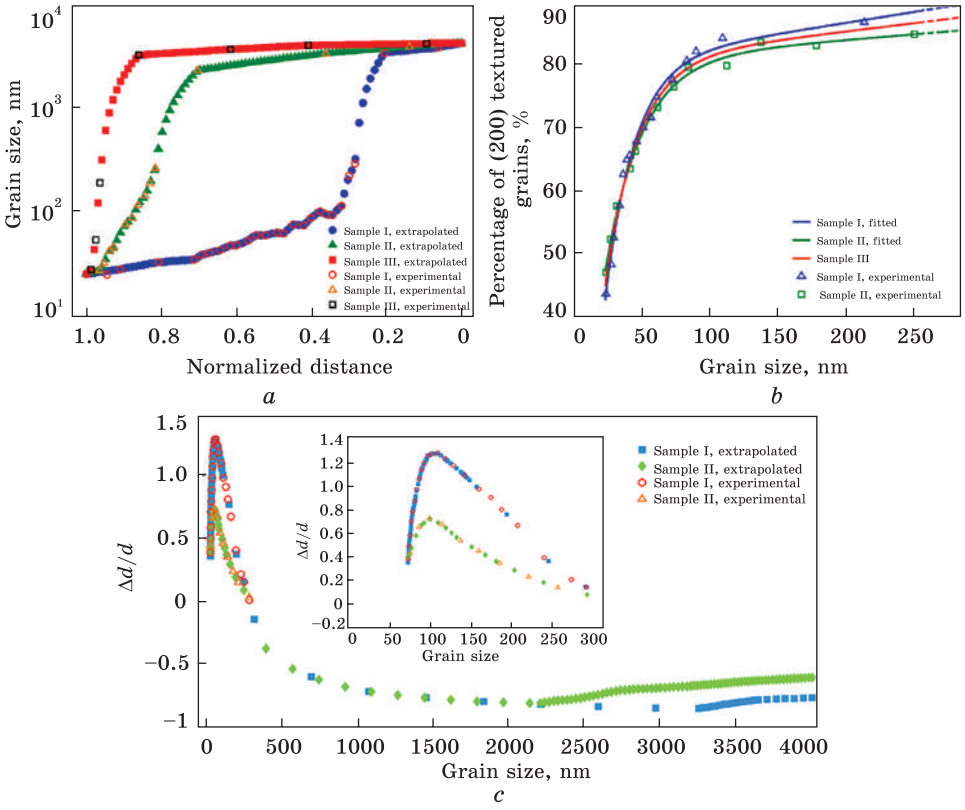

Fig. 7. Engineering strain curves of the graded nanostructured Ni samples I, II, and III under uniaxial tension predicted within the model as compared with experimental data adopted from Refs. [62, 63]. Here, *a* — grain size gradients, *b* — texture gradients, and *c* — grain growth capacity gradients. Hollow symbols — experimental data; solid symbols — their extrapolated values used in the simulations. Solid lines (*b*) — the texture gradients determined through fitting the experimental data; dashed lined (*b*) — their extrapolations. Due to the absence of experimental data, the texture gradient of sample III is obtained from the calculations of the average values of those for samples I and II. Enlarged view of the grain growth capacity gradients of samples I and II with the grain sizes <280 nm is contained in the inset (*c*) [53]

do not have a one-to-one correspondence with higher-level models in terms of shape, size, and location of each grain [53]. The nodal degrees of freedom (NDF) on faces RD, TD, and ND are constrained along RD, TD, and ND, respectively. Uniaxial tension is applied to the RD + surface along RD at a constant strain rate [53].

The authors of Ref. [62] obtained samples of pure Ni having a gradient structure with a grain size change of up to three orders of magnitude from 29 nm to 4 μm by electrodeposition, where the degree of grain size is precisely controlled. Graded Ni specimens show a favourable

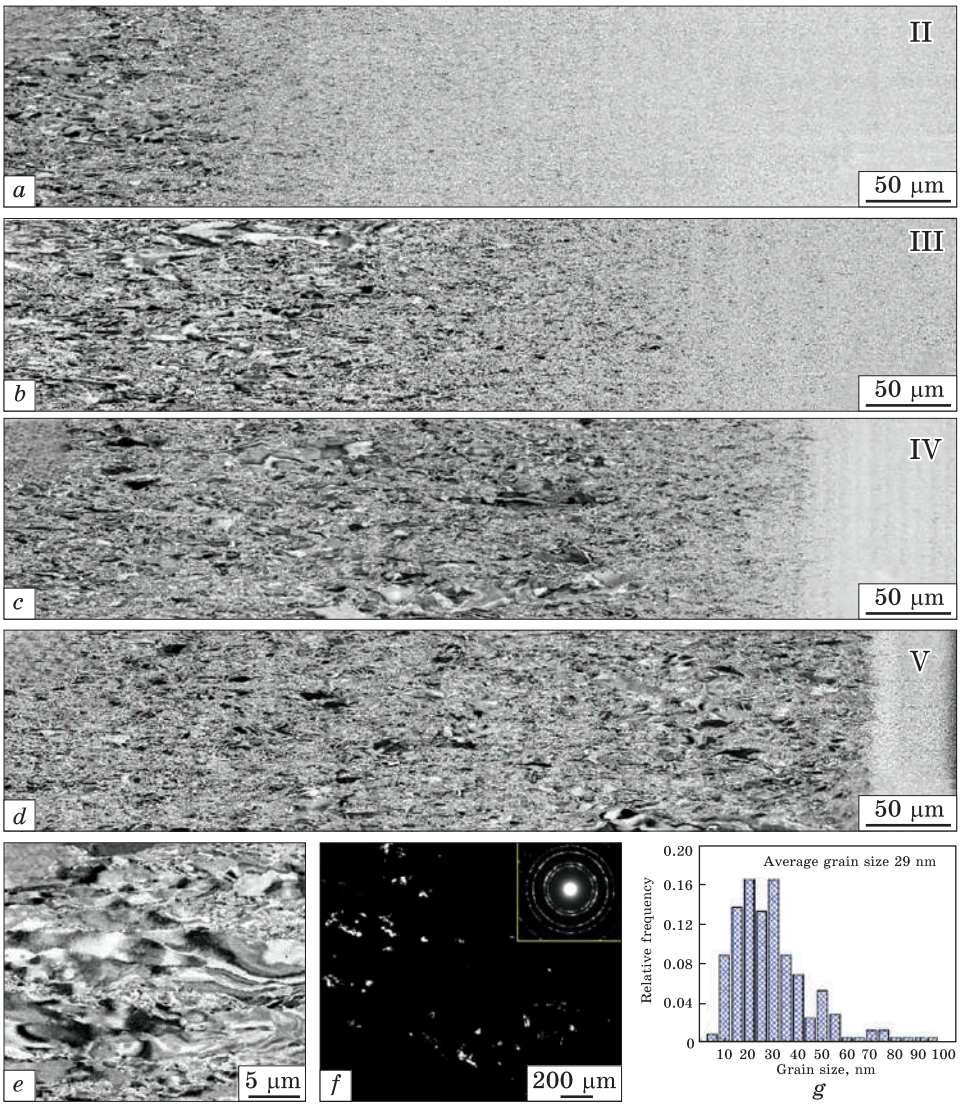

Fig. 8. Gradient structures of Ni plates after hard facing (*a*–*d*) — SEM cross-sectional images of the samples II, III, IV, and V, respectively; *e* — representative SEM image of large grains on the coarse grained side; *f* — dark-field TEM image, and *g* — corresponding particle size distribution of the uppermost surface layer from the nanograined side [62]

combination of high strength and high ductility. The optimal particle-size distribution profile provides yield strength of 460 MPa and a uniform elongation of 8.9%, which is even better than coarse Ni. Experimental observations and molecular dynamics simulations show that coarse grain surface roughness and nanograin-deformation localization

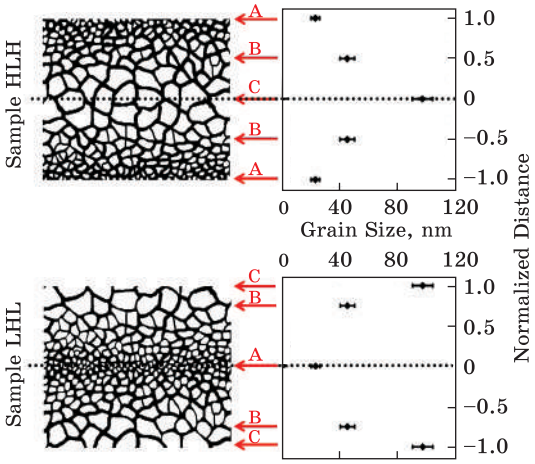

Fig. 9. Schematic patterns and plots of two series of gradient nanostructured Ni possessing symmetrical structure [64]

can be effectively suppressed by mutual confinement between nanograins and coarse grains, resulting in excellent uniform elongation. This work not only reports a promising methodology for obtaining materials with both high strength and high ductility, but also provides a model for investigating the mechanism of deformation in graded materials. The microstructure of graded Ni samples is shown in Fig. 8, *a*, *d* using cross-sectional SEM images of four graded Ni samples, i.e. samples II, III, IV, and V, respectively. In addition, a microstructural evolution of large grains to small grains along the deposition direction without a sharp interface is observed in the samples, which indicates a typical gradient structure. In all samples, grain size starts from ≈4 μm at the end of large columnar grains (Fig. 8, *e*), and gradually decreases to 29 nm closer to the end of small grains (Fig. 8, *f*, *g*). The range of grain size variation covers almost three orders of magnitude. Moreover, change in the size of finer grains is much more gentle in sample II than in sample IV, resulting in a higher proportion of nanograins. This indicates a clear difference in the degree of grain size gradient in samples II and IV.

The authors of the article [64] studied the quantitative microstructural evolution and corresponding microhardness of an electrodeposited nanostructured nickel sheet during cold rolling deformation by x-ray diffraction, transmission electron microscopy, and determination of Vickers microhardness. The influence of stress states on the deformation behaviour of two types of graded nanostructured nickel was studied: with symmetrical structures and homogeneous, and analogues with three grain sizes were compared based on macrostatistical data. Figure 9 shows two series of gradient nanostructured study materials. Two samples were used: gradient with a high surface hardness, but with low core hardness — HLH, as well as a gradient sample with a low surface hardness, but with high core hardness — LXL. Based on the electrodeposition rate, it can be calculated that layer B is located 1/4 of the thickness from the surface of the HLH sample and 1/8 of the thickness from the surface of the LHL sample. In such hierarchical sandwich-shaped gradi-

ent patterns, layers with larger grain size, like the softer phase, do withstand greater deformation. Changes in grain rotation caused by deformation are observed in the central layers with relatively larger grain sizes, accompanied by an obvious decrease in microhardness. In quantitative microstructural terms including grain size, dislocation density, and stacking fault probability before and after deformation, evaluation based on Hall–Petch and Bailey–Hirsch ratios indicates the transition from work hardening to softening can be explained by a change in grain orientation.

6. Ceramic Functional-Gradient Materials

Functionally graded materials (FGM) are composite or single-phase materials, functional properties of which change uniformly or abruptly along a predetermined and developed profile [65–67]. The property change profile, in turn, is due to the heterogeneity of microstructure, the design of which is determined by the requirements for the performance characteristics of the final product. Due to the gradual transition from one material to another in the FGM, abrupt changes in the properties that exist in the composite material are eliminated.

Thus, FGM have a combination of properties that differ from the properties of the original structural elements and allow the material to be adapted to the required application conditions. The main task of FGM design is to combine incompatible functionality in one product. Functionally graded structures are found in nature, such as bones, teeth, wood, etc. [68, 69]. FGM was first used in the mid-1980s by Japanese researchers working on a new aircraft project. The material they created made it possible to work at very high temperatures (≈1700 °C), with a temperature gradient of approximately 1000 °C over a thickness of 10 mm. This can be achieved by gradually changing the phase composition (creating a gradient) of the thermal barrier coating (ZrO_2/NiCoCrAl) [70].

The interest in FGM is caused, first, by the prospects of their practical application, for example, in thermal protection systems, for oxidation- and corrosion-resistant barrier coatings that can withstand large temperature gradients, in the design of engine components for aviation and space technology, and in nuclear reactors [71]. FGM is also used to compensate for the difference in thermal coefficients of linear expansion (TCLE) of the materials being joined. For instance, when joining ceramics and metal through the intermediate gradient layer, with a modified TCLE, the stresses are not concentrated at the interface, but are distributed in the intermediate layer, preventing cracking of the part. FGM can be used to replace living tissue from compatible materials such as bones and teeth. The ability to prevent the propagation of cracks

makes the use of FGM useful as personal protective equipment. FGM are also promising for application in the energy conversion devices.

The main goal of creating FGM is to implement the spatial distribution of the microstructure and/or composition in the finished product. There are two types of gradient structures: continuous and stepwise. In both types, there is a change in the volume fraction of materials along a certain direction; however, in the case of the continuous type, the change in composition occurs smoothly, while the stepped gradient is characterized by sharp changes in composition (microstructure), and, consequently, properties. FGM include materials with a gradient in phase composition, porosity, and particle size distribution.

When choosing a method for manufacturing FGM, the difference between the properties of the constituent components and need to obtain a product free from macrodefects are of paramount importance. The process of creating FGM can be divided into the formation of a gradient structure and consolidation. Consolidation processes must be chosen so that the gradient structure is not destroyed or changed in an uncontrolled manner as a result of residual and thermal stresses and uneven shrinkage. The presence of stresses leads to destruction or delamination and loss of the functional qualities of FGM structures, so the problem of determining the combination of material properties and the type of gradient is relevant today. Various methods are used to obtain FGM, *e.g.*, plasma and thermal spraying, powder technology methods, physical and chemical gas-phase deposition, additive technologies, laser sintering, self-propagating high-temperature synthesis, thermal diffusion treatment, etc. There are the most widely used methods for gradient structures fabrication: thermal and plasma sputtering, electrodeposition, chemical and physical vapour deposition. These methods form an excellent microstructure, they can be used for applying thin coatings, but they are not suitable for obtaining bulk FGM due to high labour costs. In Ref. [72], gradient thermal barrier coatings (ZrO_2–NiCrAl) were obtained by plasma sputtering and their properties were studied. Spheroidized powders were used as feedstock. Coatings were made with different number of layers, each with a thickness of 100 to 200 μm. The sprayed coatings were additionally sintered by hot isostatic pressing (HIP). Tests of samples of gradient coatings have shown that after HIP, the bond strength of the coating increases significantly due to the compaction of the microstructure, the reduction of defects and mutual diffusion between layers, and reduction of residual thermal stresses. Bond strength of five-layer coatings was approximately twice that of two-layer coatings due to a smoother transition from material to material, *i.e.* a significant reduction in residual stresses. For the manufacture of bulk FGM, powder technology methods are excellent due to the wide

variety of formation and consolidation processes used. The formation of a step-by-step gradient structure is possible by placing powder materials in a mould in the order determined by the product design. Substrate casting process can be also used for this. In this case, thin sheets of the required composition are made, which are laid out in a certain sequence. Resulting workpiece can be given with desired size and shape by stamping or cutting. This process is highly productive but requires removal of the binder prior to consolidation. Consolidation of workpieces manufactured by powder technology is usually carried out by cold pressing, cold isostatic pressing (CIP) followed by sintering, hot pressing (HP), hot isostatic pressing (HIP) and spark plasma sintering. In Ref. [73], ZrB_2–SiC/ZrO_2 (3Y) system was chosen for fabrication of FGM with a stepped profile. The ZrB2–SiC system is of interest as an ultra-high temperature material due to its good thermal and corrosion resistance. Partially stabilized zirconia was used as thermal insulation. Pre-prepared powders with volume fractions of ZrO_2 (3Y) (0, 10, 30, 50, 70, and 100%) were loaded into the graphite mould layer by layer. Consolidation was carried out by spark plasma sintering at a temperature of 1850 °C. As a result, a pore-free FGM without delamination and warping was obtained. A continuous gradient structure can be obtained using centrifugal casting. The formation of the gradient occurs under the action of centrifugal forces due to the different density of the components. This method is limited in the form of products, mainly cylindrical bodies. For example, to make metal gradient tubes, the more refractory particles are dispersed into the molten metal in a centrifuge. The difference in density between particles and melt leads to the formation of a particle concentration gradient. Depending on whether it is necessary to create the highest concentration on the inner or outer surface of the tube, particles with a density of a lower or higher density of melt are introduced, respectively [51]. Great prospects for the creation of gradient materials are offered by the so-called additive technologies (3*D* printing) [74, 75]. The creation of gradient materials is carried out on the basis of a three-dimensional computer model by layer-by-layer application and fixation of several materials. For example, a turbine blade can be grown with arbitrary configurations of cooling channels, which is not possible with conventional machining methods. Methods for supplying energy for fixing the formed layer are possible by various methods, for example, using thermal action (laser, electron beam, etc.), irradiation with ultraviolet or visible light, using a binder composition, etc. At present, the directions of 3*D* printing of parts from polymer and metal materials are rapidly developing, but research is also being actively conducted on the use of additive technologies for the manufacture of ceramic parts. However, 3*D* printing can already be used to form a gradient structure from ceramic materials for its subsequent consoli-

dation, for example, by spark plasma sintering. Layer-by-layer printing on a commercial 3*D* printer by extrusion of an aqueous suspension of boron carbide (B_4C) with a polymer was used to produce ceramic samples. After burning out the binders, the samples were sintered at a temperature of 2000 °C. In the obtained samples, no residual porosity or boundaries between layers were detected, which confirms possibility of using 3D printing to produce FGM even from refractory ceramics [76].

One of the specific problems in the consolidation of FGM is the formation of microdefects caused by non-uniform shrinkage during consolidation. The difference in the rate and magnitude of shrinkage of FGM components depends on their sintering temperature, initial density, powder particle size, etc. The problem becomes more serious in multilayer samples, because distortions and defects in one layer can affect other layers. This imposes restrictions on the design of the gradient structure and requires a large amount of research aimed at solving this problem. With a large difference in the sintering rate of the FGM components, it is possible to use pressure sintering (hot pressing, spark plasma sintering, hot isostatic pressing), temperature gradient during sintering, sintering in the liquid phase, laser sintering, and controlling the size of powders and porosity at formation of a gradient structure. For example, a spark-plasma sintering unit has been successfully used for the synthesis of FGM of various systems of ceramics with metals.

FGM allows you to achieve characteristics unattainable with traditional materials, which is fundamentally changing the manufacturing process in the 21st century. The main expectations from the use of products based on FGM are an increase in the operating temperature, an increase in strength, an increase in the service life of products, and, as a result, a significant saving of energy resources. Of the variety of methods for forming gradient structures, additive technologies are the most promising. Their use will help to automate production and significantly reduce the cost of manufacturing products from ceramic FGM. Formation of gradients of chemical and phase composition or microstructure is a promising area of scientific research.

7. Conclusions

Nowadays, in the modern conditions, requirements for the properties of structural materials are becoming increasingly stringent. This is especially true for materials in aerospace engineering, energy and other industries characterized by extremely unfavourable, extreme operating conditions for critical parts, structural elements and assemblies. Until recently, the widespread mandatory requirement for uniform structure (of almost any product, regardless of operating conditions and the nature of the load) seemed obvious and justified. However, in many cases,

the presence of a gradient structure allows the material to acquire new, previously unknown properties. Therefore, the growing interest in composite materials and metals with a gradient structure (GS) is natural.

It should be noted that, despite the intensive study of gradient structures, ideas about the processes of their formation and evolution are not well described, and the corresponding scientific direction is at the stage of intensive accumulation and comprehension of factual (experimental) and theoretical material. This circumstance hinders the development and implementation of new modern technologies. In this regard, the establishment of regularities and mechanisms for the formation of gradient structural–phase states in steels of various structural classes and purposes determines the relevance and prospects of research in this area.

Acknowledgement. This study is supported by the Science Committee of the Ministry of Science and Higher Education of the Republic of Kazakhstan (Grant No. AP19678974).

REFERENCES

1. I.E. Volokitina, A.V. Volokitin, M.A. Latypova, V.V. Chigirinsky, and A.S. Kolesnikov, *Prog. Phys. Met.*, **24**, No. 1: 132–156 (2023); https://doi.org/10.15407/ufm.24.01.132
2. S.Y. Hong, *Machining Sci. Technol.*, **10**, No. 1: 133 (2006); https://doi.org/10.1080/10910340500534324
3. A. Bychkov and A. Kolesnikov, *Metallogr. Microstruct. Anal.*, **12**, No. 3: 564–566 (2023); https://doi.org/10.1007/s13632-023-00966-y
4. S.M. Yuan, L.T. Yan, W.D. Liu, and Q. Liu, *J. Mater. Process. Technol.*, **211**, No. 3: 356–362 (2011); https://doi.org/10.1016/j.jmatprotec.2010.10.009
5. I.E. Volokitina and A.V. Volokitin, *Metallurgist*, **67**: 232–239 (2023); https://doi.org/10.1007/s11015-023-01510-7
6. B. Sapargaliyeva, A. Agabekova, G. Ulyeva, A. Yerzhanov, and P. Kozlov, *Case Studies in Construction Materials*, **18**: e02162 (2023); https://doi.org/10.1016/j.cscm.2023.e02162
7. R.Z. Valiev, A.V. Sergueeva, and A.K. Mukherjee, *Scripta Mater*, **49**, No. 7: 666–674 (2003); https://doi.org/10.1016/S1359-6462(03)00395-6
8. M. Hawryluk, J. Ziemba, and P. Sadowski, *Mater. Sci.*, **50**, No. 3: 74–78 (2017); https://doi.org/10.1177/0020294017707161
9. N. Vasilyeva, R. Fediuk, and A. Kolesnikov, *Materials*, **15**: 3975 (2022); https://doi.org/10.3390/ma15113975
10. P. Wang, L. Zhao, J. Liu, M.D. Weir, X. Zhou, and H.H.K. Xu, *Bone Research.*, **2**: 14017 (2014); https://doi.org/10.1038/boneres.2014.17
11. I.E. Volokitina, A.V. Volokitin, and E.A. Panin, *Prog. Phys. Met.*, **23**, No. 4: 684–728 (2022); https://doi.org/10.15407/ufm.23.04.684

12. D.A. Hughes and N. Hansen, *Phys. Rev. Lett.*, **87**, No. 13: 135503 (2001); https://doi.org/10.1103/PhysRevLett.87.135503
13. T.H. Fang, W.L. Li, and N.R. Tao, *Science*, **331**, No. 6024: 1587–1590 (2011); https://doi.org/10.1126/science.1200177
14. I.E. Volokitina, *Metal Sci. Heat Treat.*, **62**: 253–258 (2020); https://doi.org/10.1007/s11041-020-00544-x
15. K. Lu, *Science*, **345**, No. 6203: 1455–1456 (2014); https://doi.org/10.1126/science.1255940
16. X.L. Wu, P. Jiang, and L. Chen, *Mater. Res. Lett.*, **2**, No. 4: 185–191 (2014); https://doi.org/10.1080/21663831.2014.935821
17. Y.J. Wei, Y.Q. Li, and L.C. Zhu, *Nat. Commun.*, **5**: 3580 (2014); https://doi.org/10.1038/ncomms4580
18. G.I. Raab, L.A. Simonova, and G.N. Alyoshin, *Metalurgija*, **55**: 177–180 (2016).
19. B. Ilschner, *J. de Physique IV Proc.*, **3**: C7-763–C7-772 (1993); https://hal.science/jpa-00251740
20. M.B. Bever and P.E. Duwez, *Mater. Sci. Eng.*, **10**: 1–8 (1972); https://doi.org/10.1016/0025-5416(72)90059-6
21. M. Shen and M.B. Bever, *J. Mater. Sci.*, **7**: 741–746 (1972); https://doi.org/10.1007/BF00549902
22. C. Olin, L. Durant, N. Favrot, J. Besson, G. Barrbier, and F. Dellanay, *Proc. 13th Int. Plansee Seminar (24–28 May 1993, Plansee, Austria)* (Ed. H. Bildstein and R. Eck), p. 522–536.
23. M. Danilenko and V. Gorban, *Materials Science Forum*, **503**: 787–792 (2006); https://doi.org/10.4028/www.scientific.net/MSF.503-504.787
24. S. Ramesh Kumar, K. Gudimetla, B. Tejaswi, and B. Ravisankar, *Trans. Indian. Inst. Met.*, **70**: 639–648 (2017); https://doi.org/10.1007/s12666-017-1073-2
25. I.E. Volokitina, *Metal Sci. Heat Treat.*, **61**: 234–238 (2019); https://doi.org/10.1007/s11041-019-00406-1
26. K.O. Kostyk, V.O. Kostyk, and V.D. Kovalev, *Prog. Phys. Met.*, **22**, No. 1: 78 (2021); https://doi.org/10.15407/ufm.22.01.078
27. H. Tian, H.L. Suo, O.V. Mishin, Y.B. Zhang, D. Jensen, and J.-C. Grivel, *J. Mater. Sci.*, **48**: 4183–4190 (2013); https://doi.org/10.1007/s10853-013-7231-y
28. E.V. Galieva, V.A. Valitov, R.Ya. Lutfullin, and A.A. Bikmukhametova, *Defect Diffus. Forum*, **385**: 150–154 (2018); https://doi.org/10.4028/www.scientific.net/DDF.385.150
29. M. Kawasaki, B. Ahn, H.J. Lee, A.P. Zhilyaev, and T.G. Langdon, *J. Mater. Res.*, **31**: 88–99 (2016); https://doi.org/10.1557/jmr.2015.257
30. A.V. Volokitin, I.E. Volokitina, and E.A. Panin, *Prog. Phys. Met.*, **23**, No. 3: 411–437 (2022); https://doi.org/10.15407/ufm.23.03.411
31. A.P. Zhilyaev, G. Ringot, Y. Huang, J.M. Cabrera, and T.G. Langdon, *Mater. Sci. Eng. A*, 688: 498 (2017); https://doi.org/10.1016/j.msea.2017.02.032
32. G. Langford and M. Cohen, *Trans. ASM*, **62**: 623–637 (1969);
33. V.M. Segal, *Mat. Sci. Eng. A*, **338**: 331–344 (2002); https://doi.org/10.1016/S0921-5093(02)00066-7

34. Y. Beygelzimer, V. Varyukhin, D. Orlov, B. Efros, A. Salimgareyev, and V. Stolyarov, *Ultrafine Grained Materials: Processing and Structure* (Washington: 2002), pp. 137–142.
35. A.W. Thompson, *Met. Trans. A*, **7**: 833–842 (1977); https://doi.org/10.1007/bf02661564
36. V. Rybin, *Zakonomernosti Formirovaniya Mezostruktur v Khode Razvitoy Plasticheskoy Deformatsii* [Regularities of Mesostructure Formation during Developed Plastic Deformation] (Materials Science: 2002) (in Russian).
37. N.I. Noskova and A.V.Korznikov, *Phys. Metals Metallogr.*, **94**: 24–29 (2002).
38. M. Nemoto, Z. Horita, M. Furukawa, and T.G. Langdon, *Mater. Sci. Forum*, **304–306**: 59–66 (1999); https://doi.org/10.4028/www.scientific.net/msf.304-306.59
39. A.V. Belotskii and A.I. Yurkova, *Metallofiz. Noveishie Tekhnol.*, **23**, No. 4: 551–557 (2001).
40. A. Dzubenko, A. Lapunov, and I. Radomiselsky, *Powder Metallurgy*, **9**: 43–48 (1986); https://doi.org/10.1016/0026-0657(93)92883-7
41. S. Takaki, *Mater. Sci. Forum*, **426–432**: 215–222 (2003); https://doi.org/10.4028/www.scientific.net/MSF.426-432.215
42. N. Tao, Z. Wang, W. Tong, M. Sui, J. Lu, and K. Lu, *Acta Mater.*, **50**, No. 18: 4603–4616 (2002); https://doi.org/10.1016/S1359-6454(02)00310-5
43. K. Lu and J. Lu, *Mater. Sci. Eng. A*, **375–377**: 38–45 (2004); https://doi.org/10.1016/j.msea.2003.10.261
44. A. Naizabekov, A. Volokitin, and E. Panin, *J. Mater. Eng. Perform.*, **28**, No. 3: 1762–1771 (2019). https://doi.org/10.1007/s11665-019-3880-6
45. W. Tong, N. Tao, Z. Wang, J. Lu, and K. Lu, *Science*, **299**, No. 5607: 686–688 2003; https://doi.org/10.1126/science.1080216
46. I. Volokitina, A. Volokitin, A. Denissova, Y. Kuatbay, and Y. Liseitsev, *Case Studies in Construction Materials*, **19**: e023462023; https://doi.org/10.1016/j.cscm.2023.e02346
47. N. Zhangabay, B. Sapargaliyeva, U. Suleimenov, K. Abshenov, A. Utelbayeva, A. Kolesnikov, K. Baibolov, R. Fediuk, D. Arinova, B. Duissenbekov, A. Seitkhanov, and M. Amran, *Materials*, **15**: 5732 (2022) https://doi.org/10.3390/ma15165732
48. T. Tursunkululy, N. Zhangabay, U. Suleimenov, K. Abshenov, A. Utelbayeva, A. Moldagaliyev, Z. Turashova, G. Karshyga, and P. Kozlov, *Case Studies in Construction Materials*, **18**: e02019 (2023); https://doi.org/10.1016/j.cscm.2023.e02019
49. S.M. Hassani-Gangaraj, K.S. Cho, H.J.L. Voigt, M. Guagliano, and C.A. Schuh, *Acta Mater.*, **97**: 105–115 (2015); https://doi.org/10.1016/j.actamat.2015.06.054
50. O. Kolesnikova, N. Vasilyeva, A. Kolesnikov, and A. Zolkin, *Mining Inf. Anal. Bull.*, **10**, No. 1: 103–115 (2022); https://doi.org/10.25018/0236_1493_2022_101_0_103
51. G.I. Raab and R.Z. Valiev, *Non-Ferrous Metallurgy*, **5**: 50–53 (2000).
52. A.G. Raab, A.P. Zhilyaev, I.S. Kodirov, and G.N. Aleshin, *Mater. Sci. Non-Equilibrium Phase Transformations*, **1**: 11–12 (2019).
53. R. Yuan, *Acta Mechanica*, **234**: 4147–4181 (2023); https://doi.org/10.1007/s00707-023-03606-2

54. V.A. Tatarenko, T.M. Radchenko, A.Yu. Naumuk, and B.M. Mordyuk, *Prog. Phys. Met.*, **25**, No. 1: 3–26 (2024);
https://doi.org/10.15407/ufm.25.01.003
55. D.S. Leonov, T.M. Radchenko, V.A. Tatarenko, and Yu.A. Kunitsky, *Defect Diffus. Forum*, **273–276**: 520–524 (2008);
https://doi.org/10.4028/www.scientific.net/DDF.273-276.520
56. T.M. Radchenko and V.A. Tatarenko, *Defect Diffus. Forum*, **273–276**: 525–530 (2008);
https://doi.org/10.4028/www.scientific.net/DDF.273-276.525
57. P. Szroeder, I.Yu. Sagalianov, T.M. Radchenko, V.A. Tatarenko, Yu.I. Prylutskyy, and W. Strupiński, *Appl. Surf. Sci.*, **442**: 185–188 (2018);
https://doi.org/10.1016/j.apsusc.2018.02.150
58. P. Szroeder, I. Sahalianov, T. Radchenko, V. Tatarenko, and Yu. Prylutskyy, *Optical Mater.*, **96**: 109284 (2019);
https://doi.org/10.1016/j.optmat.2019.109284
59. A.G. Solomenko, R.M. Balabai, T.M. Radchenko, and V.A. Tatarenko, *Prog. Phys. Met.*, **23**, No. 2: 147–238 (2022);
https://doi.org/10.15407/ufm.23.02.147
60. A.G. Solomenko, I.Y. Sahalianov, T.M. Radchenko, and V.A. Tatarenko, *Sci. Rep.*, **13**: 13444 (2023);
https://doi.org/10.1038/s41598-023-40541-7
61. O.S. Skakunova, S.I. Olikhovskii, T.M. Radchenko, S.V. Lizunova, T.P. Vladimirova, and V.V. Lizunov, *Sci. Rep.*, 13, 15950 (2023);
https://doi.org/10.1038/s41598-023-43269-6
62. Y. Lin, J. Pan, H.F. Zhou, H.J. Gao, and Y. Li, *Acta Mater.*, **153**: 279–289 (2018);
https://doi.org/10.1016/j.actamat.2018.04.065
63. Y. Lin, J. Pan, Z. Luo, Y. Lu, K. Lu, and Y. Li, *Nano Mater. Sci.*, **2**, No. 1: 39–49 (2020);
https://doi.org/10.1016/j.nanoms.2019.12.004
64. H. Ni, L. Wang, Zh. Wang, and J. Zhu, *Rev. Adv. Mater. Sci.*, **59**: 144–150 (2020);
https://doi.org/10.1515/rams-2020-0105
65. P. Shanmugavel, G.B. Bhaskar, M. Chandrasekaran, P.S. Mani, and S.P. Srinivasan, *Eur. J. Sci. Res.*, **68**. No. 3: 412–439 (2012);
66. B. Kieback, A. Neubrand, and H. Riedel, *Mater. Sci. Eng. A*, **362**, Nos. 1–2: 81–105 (2003);
https://doi.org/10.1016/S0921-5093(03)00578-1
67. T. Liu, Q. Wang, A. Gao, C. Zhang, C.J. Wang, and J.C. He, *Scripta Mater.*, **57**, No. 11: 992–995 (2007);
https://doi.org/10.1016/j.scriptamat.2007.08.011
68. T. Knoppers, J.W. Gunnink, J. Van den Hout, and W. Van, *TNO Science and Industry*, p. 38–43.
69. J.J. Lannutti, *Composites Engineering*, **4**, No. 1: 81–94 (1994);
https://doi.org/10.1016/0961-9526(94)90010-8
70. M. Niino, T. Hirai, and R. Watanabe, *J. Jap. Soc. Compos. Mat.*, **13**: 257–264 (1987);
https://doi.org/10.6089/jscm.13.257
71. L. Marin, *Int. J. Solids Struct.*, **42**, No. 15: 4338–4351 (2005);
https://doi.org/10.1016/j.ijsolstr.2005.01.005

72. Y.W. Gu, K.A. Khor, Y.Q. Fu, and Y. Wang, *Surf. Coat. Technol.*, **96**, Nos. 2–3: 305–312 (1997);
https://doi.org/10.1016/S0257-8972(97)00185-0
73. C.Q. Hong, X.H. Zhang, W.J. Li, J.C. Han, and S.H. Meng, *Mater. Sci. Eng. A*, **498**, Nos. 1–2: 437–441 (2008);
https://doi.org/10.1016/j.msea.2008.08.032
74. L.J. Zhang, Y.-Q. Wang, B.L. Zhou, and X.-Q. Wu, *J. Mater. Sci. Lett.*, **17**: 1677–1679 (1998);
https://doi.org/10.1023/A:1006635221379
75. D. Dimitrov, K. Schreve, and N. De Beer, *Rapid Prototyping J.*, **12**, No. 3: 136–147 (2006);
https://doi.org/10.1108/13552540610670717
76. J. Costakis, M.L. Rueschhoff, I. Andres Diaz-Cano, P.J. Youngblood, and W. Rodney, *J. Eur. Ceramic Society*, **36**, No. 14: 3249–3256 (2016);
https://doi.org/10.1016/j.jeurceramsoc.2016.06.002

Received 24.09.2023
Final version 16.02.2024

І.Є. Волокітіна, А.І. Денісова, А.В. Волокітін, Є.А. Панін
Карагандинський індустріальний університет,
просп. Республіки, 30,
101400 Темиртау, Казахстан

МЕТОДИ ОДЕРЖАННЯ ҐРАДІЄНТНОЇ СТРУКТУРИ

Оглянуто методи одержання функціонально-ґрадієнтних матеріалів, що мають високий комплекс унікальних механічних, технологічних і спеціальних властивостей під час роботи на удар, знос, втому, що зазнають підвищених циклічних і знакозмінних навантажень. Розглянуті матеріали застосовуються в аерокосмічній техніці, енергетиці та інших галузях, що вирізняються вкрай несприятливими екстремальними умовами експлуатації відповідальних деталів, елементів конструкцій і аґреґатів. Розглянуто різні методи одержання ґрадієнтних структур, зокрема метод інтенсивної пластичної деформації металів і процес активного вигинання міді. Вивчається вплив ґрадієнтів розміру, текстури та здатности до зростання зерна на механізми деформації та механічні властивості ґрадієнтно-наноструктурованого нікелю, а також керамічних функціонально-ґрадієнтних матеріалів. Огляд може бути цікавим дослідникам і вченим у галузі матеріалознавства, металурґії та нанотехнологій.

Ключові слова: ґрадієнтні структури, функціонально-ґрадієнтні матеріали, наноструктурні матеріали, інтенсивна пластична деформація, механічні властивості матеріалів.